

# Impedance Spectroscopy Study of a Polymer Composite with Carbon Nanotubes in Contact with an Electrolyte

I. A. Markevich<sup>a,\*</sup>, N. A. Drokin<sup>b</sup>, and G. E. Selyutin<sup>a</sup>

<sup>a</sup> Institute of Chemistry and Chemical Technology, Krasnoyarsk Scientific Center, Siberian Branch, Russian Academy of Sciences, Krasnoyarsk, 660036 Russia

<sup>b</sup> Kirensky Institute of Physics, Krasnoyarsk Scientific Center, Siberian Branch, Russian Academy of Sciences, Krasnoyarsk, 660036 Russia

\*e-mail: [4ubekpam@mail.ru](mailto:4ubekpam@mail.ru)

Received February 7, 2019; revised February 7, 2019; accepted February 12, 2019

**Abstract**—The measured frequency dependence of the electric impedance of a composite based on ultra-high molecular weight polyethylene reinforced with carbon nanotubes in contact with an electrolyte is presented. The behavior of the active and reactive impedance components, permittivity, and conductivity in the frequency range from 0.1 Hz to 120 MHz is analyzed. An equivalent electric circuit simulating the dispersion of the impedance of the polymer composite making contact with the electrolyte is proposed. The formation of a double electric layer at the interface between the polymer composite and electrolyte layer is demonstrated and the electrical characteristics of this layer are determined.

**Keywords:** impedance spectroscopy, nanotubes, electrolyte.

**DOI:** 10.1134/S1063784219090093

## INTRODUCTION

A polymer composite based on ultra-high molecular weight polyethylene reinforced with multi-walled carbon nanotubes (UHMWPE-MWCNTs) is, first of all, a lightweight, durable, and wear-resistant material with electric conductivity. The prospects for use of this composite in different fields of science and technology stimulate investigations of its structural, mechanical, and electrical properties. However, considering the high stability of UHMWPE against hostile environments, it is interesting to study the polarization and transport of electric charges at the interface between a composite and electrolytes. The established regularities of these processes and their understanding could significantly broaden the range of application of this composite in electrical engineering and electrochemistry.

The main feature of UHMWPE-MWCNTs is the percolation conductivity, in which charge transport in the bulk of the composite is implemented along conducting chains of contacting nanotubes [1]. The conductivity value depends, first of all, on the volume fraction of a conducting filler, but another important factor is the distribution of nanotubes in a dielectric matrix. The arrangement of nanotubes determines not only the through conduction of the composite, but also the mechanisms of electric polarization in the bulk of the material. Carbon nanotubes characterized by the high surface energy and entangled spatial structure are susceptible to the spontaneous formation of

aggregates, which can form random conducting clusters from tens to hundreds of microns in size in the bulk and on the surface of the polymer [2]. These clusters can be mutually polarized in an electric field and significantly affect the electrical and dielectric properties of the material.

The formation of a thin electrolyte layer between the polymer surface and one of the electrodes can evoke a sequence of electrochemical phenomena caused by the formation of a double electric layer at the electrode surface, diffusion processes, ion adsorption, etc. [3]. The polarization and transport of carriers at the interface between the UHMWPE-MWCNT composite and ionic electrolytes have not been studied yet. In this study, a method for measuring the electric impedance in a wide frequency band is used to study the processes of transport and localization of electric charges in the UHMWPE-MWCNT/electrolyte interface region.

## EXPERIMENTAL

There exist different methods for fabricating polymer composites, the most universal of which is mixing the initial components in a solvent. Due to the flexible control of the temperature regimes, this method makes it possible to obtain both conducting and dielectric composites. The UHMWPE composites with 1 wt % of MWCNTs were synthesized using the

following procedure [4]. The MWCNT powder in xylene was treated by ultrasound with an intensity of  $100 \text{ W/cm}^2$  for 30 min to form a uniform suspension. The UHMWPE powder was poured in the prepared MWCNT suspension at a temperature from  $90$  to  $130^\circ\text{C}$  and the components were further mixed in an MPW-309 homogenizer at a rotation speed of  $1000 \text{ min}^{-1}$  for 10 min to obtain a visually homogeneous state. Temperature is a decisive factor in the formation of the distribution of MWCNTs over the UHMWPE matrix. At a suspension temperature of  $90^\circ\text{C}$ , nanotubes adhere to softened polymer grains, but only on their surface. This yields a mosaic structure of contacting nanotubes in the bulk of the polymer. As was shown in [5], such a structure facilitates the formation of a great number of contacts between nanotubes, which leads to an increase in conductivity  $\sigma \sim 10^{-1} - 10^{-3} \text{ S m}^{-1}$ . At a suspension temperature of  $110^\circ\text{C}$ , the UHMWPE particles partly swell and nanotubes start penetrating into the UHMWPE grains. The conductivity of such samples lowers because of their partial isolation by a polymer layer:  $\sigma \sim 10^{-4} - 10^{-6} \text{ S m}^{-1}$ . At a suspension temperature of  $130^\circ\text{C}$ , the UHMWPE particles strongly swell and a large amount of nanotubes penetrate into the polymer structure and thereby significantly reduce the conductivity. After filtering and drying the prepared mixtures, the composite powders were formed by hot pressing at 6 MPa and  $160^\circ\text{C}$  and used to prepare disk samples for measurements with a diameter of 16 mm and a thickness of  $\sim 1 \text{ mm}$ .

To analyze the frequency spectrum of the impedance of the UHMWPE-MWCNT composite contacting an electrolyte, we chose a material with a static conductivity of  $\sigma = 1.4 \times 10^{-4} \text{ S m}^{-1}$  obtained at a component mixing temperature of  $110^\circ\text{C}$ .

The electrical properties of the composites were determined by measuring the electrical impedance in the frequency range from 0.1 Hz to 120 MHz. The impedance spectroscopy method consists in measuring the ac current passing through investigated materials and determining the dispersion of the complex impedance (impedance absolute value  $|Z|$ ) and phase  $\varphi$ . Then, real impedance component  $Z'(f) = |Z|\cos\varphi$  and imaginary impedance component  $Z''(f) = |Z|\sin\varphi$  are calculated. The main goal of the impedance measurements is the search for an equivalent ac electric circuit the impedance of which would adequately simulate the experimental impedance spectra of a material under study. The individual elements of this circuit or their combination can then be compared with the physical features of the conductivity and polarity of both the composite sample and the interface between the composite surface and electrolyte.

To measure impedance  $|Z|$  and phase  $\varphi$ , thin indium electrodes with a very low transient resistance were pressed to the end surfaces of the composite samples. A measuring cell with a sample was connected to an Elins Z-1500J impedance meter operating in the

low-frequency range ( $0.01 \leq f \leq 1 \text{ MHz}$ ) and then to the ports of an E5061B spectrum analyzer for impedance measurements at frequencies up to  $f \sim 120 \text{ MHz}$ . First, the frequency dependence of the impedance absolute value and phase of the initial composite samples with indium electrodes pressed against their opposite ends was recorded on an electronic data storage device. At the next stage, a similar recording of the impedance and phase absolute values was performed with an electrolyte-impregnated capacitor paper inserted between one of the electrodes and the end sample surface. A 25% aqueous solution of NaCl was used as an electrolyte. In addition, trial recordings of the impedance spectra with adding boric acid to the salt electrolyte were performed and electrolytes of more complex compositions were tested. All the impedance spectra obtained were almost identical and are presented below.

### ELECTRICAL CHARACTERISTICS OF THE COMPOSITE

We investigated a UHMWPE-MWCNT composite sample obtained at a temperature of  $t = 110^\circ\text{C}$  of mixing initial components with a static conductivity of  $\sigma = 1.4 \times 10^{-4} \text{ S m}^{-1}$ . The frequency dependence of the impedance of this sample with indium contacts was measured in the frequency range from 100 Hz to 120 MHz, since, at lower frequencies, the phase angle approaches zero and the calculation of the dielectric characteristics of the sample becomes incorrect. The obtained spectra of the real (1) and imaginary (2) components of the sample impedance are shown in Fig. 1.

It can be seen in Fig. 1 that the initial values of the real component of impedance  $Z'(f) = 3.2 \times 10^4 \Omega$  (1) is almost frequency-independent, but, as the frequency increases, the impedance decreases to  $Z = 19 \Omega$ . At a frequency of  $f = 500 \text{ kHz}$ , the imaginary component of the impedance (2) has a pronounced relaxation maximum. The inset in Fig. 1 shows an impedance hodograph built in the Nyquist coordinates ( $Z''(f)$  vs  $Z'(f)$ ). Each hodograph point corresponds to a certain frequency counted from the right-hand side of the hodograph. Building the impedance hodograph helps find a circuit with the impedance that should approximate the measured impedance spectrum of the sample over the entire frequency range. It can be seen that this hodograph has the shape of a symmetric semicircle with the center near the  $Z'(f)$  axis. Such a hodograph is usually implemented in relatively homogeneous materials with constant resistance  $R$ , capacitance  $C$ , and relaxation time  $\tau = RC$ . However, to ensure a more accurate approximation of the hodograph and  $Z'(f)$  and  $Z''(f)$  dependences in the equivalent electric circuit shown in Fig. 1, instead of a capacitor, it is better to use a special artificial frequency-dependent element designated as a constant phase element (CPE). This specific ele-

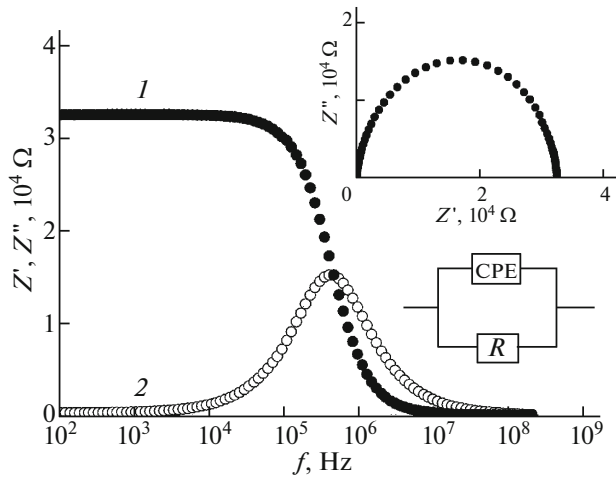


**Fig. 1.** Frequency dependences of the real (1) and imaginary (2) components of the impedance of the UHMWPE-MWCNT composite. Inset: impedance hodograph.

ment considers the nonuniform capacitance and resistance distributions over the volume of the material, is characterized by both real and imaginary impedance components, and has form [6]

$$Z_{CPE} = \frac{1}{A(j\omega)^\alpha} = \frac{1}{A\omega^\alpha} \left( \cos \alpha \frac{\pi}{2} - j \sin \alpha \frac{\pi}{2} \right), \quad (1)$$

where  $A$  is the proportionality coefficient,  $j$  is the imaginary unit, and  $0 < \alpha < 1$  is the exponent that formally characterizes a heterogeneous structure of the investigated material. The values of this equivalent circuit were numerically calculated using the EIS Spectrum Analyzer program. The determined coefficient  $A = 2.7 \times 10^{-11}$  and exponent  $\alpha = 0.94$  suggest that this CPE can be compared with the frequency-dependent capacitance specified by coefficient  $A$  and exponent  $\alpha$ . In fact, this capacitance is caused by the accumulation and relaxation of charges for an electric field half-period at the boundaries of conducting conglomerates separated by a polymer layer. These charge accumulations partially screen the external electric field, which is observed in the experiment as an apparent low-frequency increase in the capacitance and permittivity according to the Maxwell–Wagner mechanism. The complex permittivity and conductivity components are calculated using formulas [7]

$$\begin{aligned} \epsilon'_{\text{eff}} &= \frac{-Z''}{\omega C_0 (Z'^2 + Z''^2)}, \\ \epsilon''_{\text{eff}} &= \frac{Z'}{\omega C_0 (Z'^2 + Z''^2)}, \end{aligned} \quad (2)$$

$$\sigma' = Y' \frac{d}{S}, \quad \sigma'' = Y'' \frac{d}{S}. \quad (3)$$

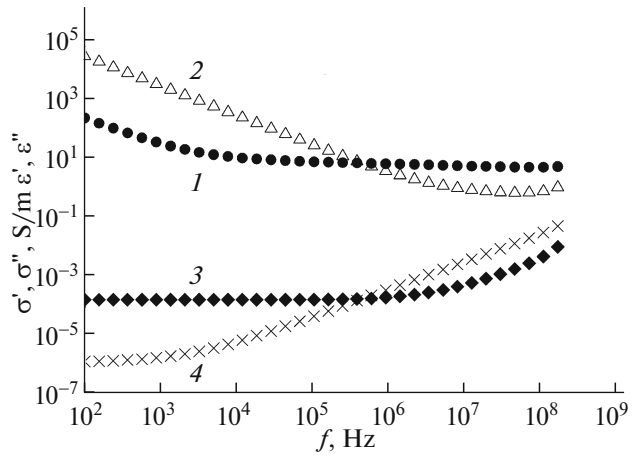


**Fig. 2.** Frequency dependences of the real (1) and imaginary (2) parts of the permittivity (3) and conductivity (4) of the UHMWPE-MWCNT composite with metal electrodes.

Here,  $\omega$  is the circular frequency;  $C_0$ ,  $d$ , and  $S$  are the geometric capacitance, thickness, and area of the measuring cell plates; and  $Y'$  and  $Y''$  are the real and imaginary components of the admittance. For the investigated sample, the frequency dependences of real ( $\epsilon'$ ) and imaginary ( $\epsilon''$ ) parts of the permittivity and real ( $\sigma'$ ) and imaginary ( $\sigma''$ ) parts of the conductivity calculated using Eqs. (2) and (3) are shown in Fig. 2.

At a frequency of  $f = 100$  Hz, the real part of the permittivity (1) attains  $\epsilon' \approx 200$  and decreases with increasing frequency to  $\epsilon' \approx 4.6$ . At a frequency of 100 Hz, the imaginary part of the permittivity (2) attains an enormous value of  $\epsilon'' = 2 \times 10^4$  and, with increasing frequency, monotonically decreases to  $\epsilon'' = 0.7\text{--}0.9$ . The growth of the real part of the permittivity in the low-frequency region is typical of such structured composites, since electric charges are accumulated in the bulk of the composite at the interfaces between the conducting and insulating regions. These charges partially screen the external electric field and lead to the apparent permittivity growth. As the electric field frequency increases, the charge accumulation weakens and the permittivity approaches a stationary value. The growth of the imaginary part of the permittivity (2) in the low-frequency region is determined by active conductivity component  $\epsilon''(f) = \sigma'(f)/(2\pi f \epsilon_0)$  [8], where  $\epsilon_0$  is the permittivity of free space. The frequency dependences of the real and imaginary parts of the conductivity are shown in Fig. 2 (3, 4). It can be seen that, up to a frequency of  $f \approx 1$  MHz, conductivity value  $\sigma'(f) = 1.4 \times 10^{-4} \text{ S m}^{-1}$  is almost frequency-independent, but, with a further increase in frequency, the conductivity monotonously grows. The high-frequency growth of the conductivity is usually explained by the hopping charge transport [9, 10] or the high-frequency relaxation conductivity caused by the delay of charge transport in an electric

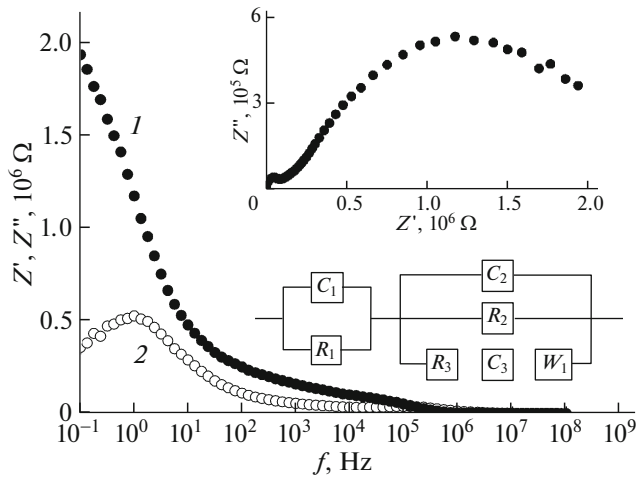


**Fig. 3.** Frequency dependences of the real (1) and imaginary (2) components of the impedance of the UHMWPE-MWCNT composite contacting with the electrolyte.

field within individual clusters [11]. In this case, the increase in conductivity can be approximated by a power frequency dependence according to empirical relation  $\sigma'(\omega) = \sigma'_0 + K\omega^s$  with a coefficient of  $K = 2 \times 10^{-11}$  and an exponent of  $s = 0.92$ .

#### ELECTRICAL CHARACTERISTICS OF THE COMPOSITE MAKING CONTACT WITH AN ELECTROLYTE

When an ac voltage is applied to a measuring cell with an electrolyte layer between the metal electrode and composite surface, the electric impedance will be determined, to a great extent, by the polarization and charge exchange between electrolyte ions and nanotube electrons. Since nanotubes are nonuniformly distributed over the polymer surface, the interface between the composite and electrolyte can be considered as a fractal set of contacts of the electrolyte with nanotubes. If a double electric layer is formed on these contacts, then it should be highly inhomogeneous, as the diffusion region adjacent to this layer. Figure 3 shows the measured frequency dependence of the real and imaginary parts of the impedance of the composite sample contacting the electrolyte in the frequency range from 0.1 Hz to 120 MHz.

It can be seen in Fig. 3 that, in the low-frequency region, the real part of the impedance (1) drastically increases and the relaxation maximum of the imaginary part of the impedance (2) shifts to a frequency of  $f \sim 1$  Hz. The shape of the impedance hodograph (inset in Fig. 3) also strongly changed. At the origin of hodograph coordinates, one can see a small semi-circumference arc formed by high-frequency ( $f \geq 1 \times 10^5$  Hz) impedance components  $Z'(f)$  and  $Z''(f)$ . This arc reflects mainly the volume characteristics of the polymer composite. The large semi-circumference arc in

the lower-frequency region arises due to the combination of phenomena at the interface between the composite and the electrolyte. To identify them, the same figure shows an electric circuit whose impedance well approximates the experimental spectra and impedance hodograph shown in Fig. 3

The equivalent circuit consists of two series-connected links. One link contains parallel-connected capacitance  $C_1$  and resistance  $R_1$  and is intended for approximating the small semi-circumference arc. The second link of the circuit simulates the region of the interface between the electrolyte and the sample surface. This part of the circuit contains capacitance  $C_2$  of the double electric layer, which occurs in an electric field at the interface between the polymer and electrolyte. The kinetics of formation and recharging of this double layer is controlled, as a rule, by the diffusion of ions, which levels their concentration in the electrolyte volume. To simulate this process, a specific Warburg element (W) was introduced into the equivalent circuit [12]. In Fig. 3, this element is located in the lower circuit of the equivalent circuit with series-connected capacitor  $C_3$  and resistance  $R_3$ . These two elements consider the additional capacity and resistance of ions adsorbed on the polymer surface and enhance the accuracy of approximation of the experimental data. The frequency dependence of the real and imaginary parts of the Warburg element is calculated using relations

$$\operatorname{Re} Z_W(\omega) = \frac{W_A}{\omega^{0.5}}, \quad \operatorname{Im} Z_W(\omega) = \frac{W_A}{\omega^{0.5}}, \quad (4)$$

where  $W_A$  is the Warburg coefficient ( $\Omega \text{ s}^{-0.5}$ ). This behavior of real and imaginary components of the impedance is caused by the fact that the uniform double electric layer forming with a decrease in frequency increasingly blocks the charge transport to the external electric circuit and causes the charge accumulation at the metal electrode. This leads to a proportional increase in both the real and imaginary components of the impedance; therefore, the straight hodograph beam makes an angle of  $45^\circ$  with the coordinate axes. However, as can be seen in Fig. 3, the straight hodograph portion that forms in the beginning is bent with a decrease in frequency, which is mainly due to the stop of the growth of the reactive (capacitive) part of the impedance. This behavior of the impedance hodograph probably originates from the structural nonuniformity of the nanotube distribution over the sample surface, which disintegrates the double electric layer and contributes to the charge transport from the electrolyte ions to the external electric circuit. Therefore, to approximate the bent hodograph beam to the equivalent circuit shown in Fig. 3, shunt resistor  $R_2$  was introduced, which simulates the current leakage through the double electric layer. This allows us to approximate the impedance hodograph by the given equivalent circuit with

**Table 1.** Values of the equivalent circuit elements (Fig. 3)

Element	Value
$R_1$	75690 $\Omega$
$C_1$	$1.37 \times 10^{-11}$ F
$C_2$	$2.80 \times 10^{-10}$ F
$R_2$	$2.0 \times 10^6$ $\Omega$
$R_3$	56700 $\Omega$
$C_3$	$3.20 \times 10^{-7}$ F
$W_A$	$3.1 \times 10^6$ $\Omega$ s <sup>-0.5</sup>

good accuracy. The obtained values of the equivalent circuit elements are given in Table 1.

Figure 4 shows frequency dependences of the real and imaginary parts of the permittivity and conductivity of the UHMWPE-MWCNT structure contacting the electrolyte calculated from Eqs. (2) and (3).

It can be seen that the electrolyte layer almost did not change the frequency dependence of the imaginary part of permittivity  $\varepsilon''(f)$  (Fig. 4, 2), but real part  $\varepsilon'(f)$  (1) in the low-frequency region increased by almost two orders of magnitude. This indirectly confirms the formation of a double electric layer. In addition, this is indicated by the behavior of the imaginary (reactive) part of conductivity  $\sigma''(f)$  (4), which also increased at low frequencies proportionally to an increase in  $\varepsilon'(f)$ . The real part (3) of conductivity  $\sigma'(f)$ , which characterizes the through electric current flow in the electrolyte and composite, remained almost invariable. This gives us grounds to introduce shunt resistance  $R_2$  into the equivalent electric circuit shown in Fig. 3.

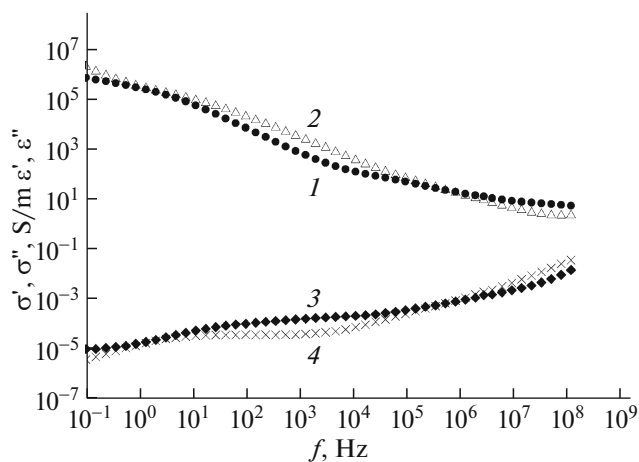


**Fig. 4.** Frequency dependences of the real (1) and imaginary (2) parts of the permittivity (3) and conductivity (4) of the UHMWPE-MWCNT composite contacting with the electrolyte.

Formally, the heterogeneous structure of the composite surface and double electric layer can be simulated also by a special CPE, the impedance of which is calculated using a fractional exponent of the electric field [13]. This element formally characterizes the degree of fractality of the electric properties of the sample surface and double electric layer, which is of great importance for comparison of the experimental results obtained for different composite samples. However, in the attempts of using this element in an equivalent electric circuit, it is compared, to a greater extent, with the distributed inductance at the polymer surface rather than the distributed capacitance of the double electric layer. This can be explained by the fact that, at the chaotic distribution of the electric potential over the composite surface in the region of the electric double layer, inhomogeneous spatial regions with mutual overflow may occur. The possible existence of an inhomogeneous double electric layer in the presence of a set of ions with different charges in an electrolyte was discussed in [14].

## CONCLUSIONS

The concept of a double electric layer forming between a conducting composite and an electrolyte is universal and was used in this study to interpret the measured impedance spectra of the UHMWPE-MWCNT composite making contact with an electrolyte. It was shown that the equivalent electric circuit of this structure consists of two series-connected links. The first link describes the polarization and conductivity of the polymer composite and the second link, the processes occurring in the double electric layer and diffusion region. It was shown that the electrically nonuniform surface structure of the polymer composite leads to the inhomogeneity of the double electric layer, which is accompanied by the occurrence of a through electric current and straight hodograph beam bending in the low-frequency range.

## CONFLICTS OF INTEREST

The authors declare that they have no conflicts of interest.

## REFERENCES

1. A. V. Elets'kii, A. A. Knizhnik, B. V. Potapkin, and J.M. Kenny, *Phys.-Usp.* **58**, 209 (2015). <https://doi.org/10.3367/UFNe.0185.201503a.0225>
2. N. Hu, Z. Masuda, C. Yan, G. Yamamoto, H. Fukunaga, and T. Hashida, *Nanotechnology* **19**, 1 (2008). <https://doi.org/10.1088/0957-4484/19/21/215701>
3. N. G. Bukun and A. E. Ukshe, *Russ. J. Electrochem.* **45**, 11 (2009).
4. I. A. Markevich, G. E. Selyutin, N. A. Drokin, and B. A. Belyaev, *Zh. Sib. Fed. Univ. Tekh. Tekhnol.* **11**, 190 (2018). <https://doi.org/10.17516/1999-494X-0022>

5. M. O. Lisunova, Ye. P. Mamunya, N. I. Lebovka, and A. V. Melezhyk, *Eur. Polym. J.* **43**, 949 (2007).  
<https://doi.org/10.1016/j.eurpolymj.2006.12.015>
6. E. Barsukov and J. R. Macdonald, *Impedance Spectroscopy: Theory, Experiment, and Applications* (Wiley, Hoboken, 2005).
7. D. K. Pradhan, R. N. P. Choudhatay, and B. K. Samantaray, *Int. J. Electrochem. Sci.* **3**, 597 (2008).
8. H. Fröhlich, *Theory of Dielectrics* (Oxford Univ. Press, 1949).
9. J. C. Dyre and T. B. Schoder, *Rev. Mod. Phys.* **72**, 873 (2000).
10. S. Saha and T. P. Sinha, *Phys. Rev. B* **65**, 134103 (2002).  
<https://doi.org/10.1103/PhysRevB.65.134103>
11. A. S. Bogatin, I. V. Lisitsa, and S. A. Bogatina, *Tech. Phys. Lett.* **28**, 779 (2002).
12. B. M. Grafov and E. A. Ukshe, *Russ. Chem. Rev.* **44**, 933 (1975).
13. J. Bisquert, G. Garcia-Belmonte, P. Bueno, E. Longo, and L. O. S. Bulhões, *J. Electroanal. Chem.* **452**, 229 (1998).
14. M. V. Fedorov and A. A. Kornyshev, *Electrochim. Acta* **53**, 6835 (2008).  
<https://doi.org/10.1016/j.electacta.2008.02.065>

*Translated by E. Bondareva*